

STRUCTURE OF THE MOHO DISCONTINUITY BENEATH SOUTH KOREA FROM TRAVEL-TIME WAVEFORM ANALYSIS

Roland Gritto, Jacob E. Siegel, and Winston C. Chan

Harris Corporation

Sponsored by Air Force Research Laboratory

Contract No. FA8718-06-C-0006

ABSTRACT

The current study is intended to collect and process seismic waveform data, perform comprehensive 3-D tomographic inversions, and produce high-resolution 3-D crustal P- and S-wave velocity models for the South Korean peninsula. The current phase of our study is concerned with the analysis and archival of Korean Meteorological Administration (KMA) waveform data from 2001 through 2006 and the mapping of the Moho discontinuity beneath the South Korean Peninsula. Phase arrival information from both, velocity and accelerometer sensors were collected. The analysis included 226 events throughout the region producing a total of 6,275 phase picks including Pg, Pn, Sg/Lg, and Sn phases. A total of 3,550 P-wave and 2,725 S-wave phases were identified. Using the combination of all available velocity and accelerometer data it was possible to estimate depth locations for 198 KMA events. The hypocenters were subsequently used to derive travel-time distance curves to appraise the quality of the travel-time picks. Static corrections were calculated for each seismic station within the KMA network to remove the effects of local inhomogeneities in the vicinity of each station. After applying static corrections to the observed travel-times, refracted P-wave phases along the Moho boundary were selected from the dataset to estimate the depth and topography of the Moho discontinuity. In total, 526 Pn phases were collected from the KMA data with hypocentral distances from 130 km to over 650 km. The resulting Moho topography reveals a slightly undulating interface with a large-scale dip from north (31 km) to south (38 km) and a depth range from 32 km in the east to 39 km in the south-west. On a smaller scale, a more pronounced depression is evident in the south-central part of the mapped area, which opens to the south. The presented results are corroborated by other studies which mapped the Moho interface using surface-wave dispersion and receiver-function analysis. The present study is complementary to these earlier works, in that a different method and a different dataset generated comparable results.

OBJECTIVES

The primary objective of this research is to produce high-resolution 3-dimensional crustal P- and S-wave velocity models of the South Korean Peninsula. The structure of the crustal model will be supplemented by the derivation of a 3-D Moho interface below the peninsula. The resulting velocity and structural models will provide valuable information for regionalization and relocation studies.

RESEARCH ACCOMPLISHED

During the first part of the research, phase waveform data from the KMA were analyzed for the years 2001 through 2006. The KMA operates a dense seismic network consisting of over 80 stations with velocity and accelerometer sensors. The analyzed data consist of triggered waveforms recorded for local and regional events throughout the Korean Peninsula. Phase arrival information of these data was subsequently used to delineate the structure of the Moho interface between crust and mantle.

Korean Meteorological Administration (KMA) Waveform Data

The KMA of the Republic of Korea (ROK) operates a dense network of seismic stations throughout the country. The network consists of 85 stations comprised of velocity and accelerometer sensors. Station configurations include combinations of velocity and accelerometer sensors as well as single sensor sites. The analyzed data included triggered waveforms of local and regional events from 2001 through 2006. For stations with single sensor configuration, the analyzed data were obtained from either velocity or accelerometer data, while both velocity and accelerometer data were obtained for those stations with dual sensor configuration. The intention is to improve the significance of data for stations where travel-time data from more than one instrument are available.

Travel Time Analysis of KMA Waveform Data

The analysis of the KMA waveform data produced a total of 6,275 phase picks from 226 events located throughout the Korean Peninsula. The number of located events amounts to a seismicity rate of approximately 38 events per year and confirms previous estimates for this region. Identified phases included Pg, Pn, Sg/Lg, and Sn. The number of individual identified phases amounted to 3,550 P-wave and 2,725 S-wave phases. Because the accelerometer data contain higher frequency information, epicentral distances from the events to the accelerometer stations were generally shorter than those associated with velocity stations, which helped to constrain the depth of the events. Furthermore, this approach decreased the uncertainty of the hypocenter location. Using the combination of velocity and accelerometer data, it was possible to estimate depth locations for 198 of the KMA events.

Quality control of the data was performed using travel-time-distance curves. The phase picks of the KMA data from 2001-2006 are shown in Figure 1. The travel-time of P- and S-wave phases is plotted as a function of hypocentral distance to assess the quality of the selected phase picks. The diamond-shaped symbols represent the P- and S-wave phases determined from the waveform data. The short black horizontal lines at each data point represent the relative location error for each hypocenter estimate associated with that phase pick. For each hypocenter, a relative error is calculated separately for the x-, y- and z-direction. In order to facilitate the presentation of this uncertainty, we take the relative errors for the three directions and calculate a single resulting vector, which represents the radius of a sphere around each hypocenter estimate indicating the uncertainty in its location. Therefore, the short black horizontal lines in Figure 1 represent the length of the radius of the error sphere for each hypocenter estimate. In contrast, the short black vertical lines at each data point represent the relative timing error for the event time associated with that phase pick. Considering all phase picks from velocity and accelerometer data, the average hypocentral error was reduced by 17% relative to the original hypocenters published by the KMA. The colored solid lines in Figure 1 represent the best linear fit, in a least-squares sense, through the cloud of travel-time picks. It can be seen that the fit is very good for hypocentral distances below 400 km. Although the number of events decreases for hypocentral distances beyond 400 km, the linear fit is still good at greater distances. The velocities values listed in Figure 1 are averaged P- and S-wave velocities of the crust and upper mantle as determined from the slope of the travel-time distance curves. These values are in good agreement with typical published estimates for the Korean Peninsula (Chang and Baag, 2006). If the model of a single-layered crust is employed to determine average crustal thickness from the travel-time curves in Figure 1, a value of

32 km is obtained. In comparison, Chang and Baag (2006) conducted receiver function studies based on teleseismic body wave data. They report a distribution of crustal thicknesses from 28 km in the eastern part to 35 km in the south-western part of South Korea. Therefore, the average value of 32 km, determined from the phase picks of the KMA data, appears to be a good estimate for crustal thickness, giving confidence in the obtained arrival times. A separate method to estimate Moho topography is presented in the next section.

Estimation of 3-D Moho Structure from Refracted P-waves

Two important parameters that define crustal structure are the depth and topography of the Moho boundary between crust and mantle. The topography of this interface can help to explain crustal tectonics and consequently the kinematics of wave propagation through the crust. Refracted P-wave phases along the Moho boundary can be used to estimate the depth of this interface. As can be seen in Figure 1, refracted Pn phases were observed between hypocentral distances from 130 km to over 650 km. In total, 637 Pn phases were collected from the KMA data from 2001-2006.

Before the depth and topography of the Moho could be estimated, near-station effects due to inhomogeneities in the near subsurface had to be removed from the Pn travel times. These static corrections prevent travel-time anomalies from near surface inhomogeneities to be mapped into anomalies of Moho elevation at depth. The static corrections were estimated using a least-squares approach minimizing the misfit between observed and calculated Pg travel times. The least-squares approach jointly inverted for a homogenous crustal velocity model and static correction terms at each recording station. These static corrections were subsequently subtracted from the Pn travel times before they were used to estimate Moho topography.

Several approximations have to be considered when estimating depth from travel times of refracted waves. The most important is that of a one-dimensional velocity model of a layer over a half space. In the current case, the velocity estimates for the crust and upper mantle derived from the linear fits in Figure 1 are utilized. Furthermore, it is assumed that the Moho interface is piece-wise flat over the propagation distance of each refracted phase along this boundary. With these approximations, ray theory and the principles of refraction seismology were applied to determine Moho depth and topography. For each refracted ray path, two depth-estimates for the Moho interface below the hypocenter and recording station were calculated together with the dip of the Moho interface between these two points. A maximum-likelihood approach was applied to the results of a grid search over a two dimensional depth-and-dip space to minimize the misfit between observed and calculated Pn travel times. Once the depth and dip of the Moho interface was determined below each hypocenter and recording station, the data were interpolated using an adjustable-tension continuous-curvature surface-gridding approach (Wessel and Smith, 1995). The result of the gridding is shown in Figure 2, which displays a 3-D surface plot of the Moho interface below South Korea. The emerging pattern reveals a slightly undulating interface with a large-scale dip from north (31 km) to south (38 km). On a smaller scale, a more pronounced depression is evident in the south-central part of the mapped area, which opens to the south. This low in topography reaches depth of 37-38 km. In order to place the Moho interface in spatial relation to the peninsula and its seismicity, Figure 3 shows a 3-dimensional composite plot of the Korean peninsula with the location of the KMA network at the surface (red triangles), the seismicity from 2001-2006 (green dots), the ray coverage for all P-wave phases analyzed for this time interval, and the Moho topography at depth. It should be noted that all rays are simplified as straight rays and that refracted rays have been omitted to not obscure the view of the Moho interface at depth. It can be seen that the seismicity is confined to the upper 20 km of the crust. However, for the tomography study during the second phase of this project, the rays associated with Pn phases that are refracted across the Moho interface will cover the region in the lower half of the crust.

To help associate Moho topography with the geography of South Korea, a contour plot of the Moho was generated and projected onto a map of the Korean Peninsula. The result is presented in Figure 4. In addition to the large-scale dip from north to south discussed in Figure 2, it can now be seen that the depth of the interface ranges from 32 km in the east to 39 km in the southwest. It should be noted that contours near the edges of the map are more uncertain due to the lack of ray coverage in these regions. The contour plot reinforces the previous interpretation that the main depression of the Moho is located below the south-central part of the country.

Appraisal of Moho Depth Estimates

Although the current analysis is based on the assumptions of a piece-wise flat Moho and a single crustal layer with homogeneous velocity, the obtained results are robust nevertheless. The largest error resulting from the violation of a piece-wise flat horizon might occur in the southeast corner of the map, where the Moho reaches a maximum dip of 3.1° over a short distance, which is likely to produce some curvature of the interface. The assumption of a piece-wise flat horizon would lead to a maximum depth error of 1.1 km, which is less than the estimated elevation change in that area. The error caused by a heterogeneous velocity distribution in the crust cannot be assessed, because the magnitude and complexity of velocity heterogeneity cannot be determined accurately enough at this stage of the project. However, it is possible to appraise the uncertainty in Moho depth based on the uncertainty in the velocity estimates given by the travel-time curves in Figure 1. If the largest deviations in crustal and mantle velocity are applied to the region with the steepest dip (3.1° in the south-east corner of the map), the maximum resulting depth error of the Moho interface would be 1.8 km. Again, this error is less than the estimated elevation change in this area. Therefore, the derived pattern of Moho elevation appears to be a robust estimate compared to the maximum errors based on the assumption made in this approximation.

Interpretation of Moho Topography

To interpret the Moho topography, it is necessary to incorporate the crustal tectonics of the Korean Peninsula. While the pattern of Moho topography does not mimic the general northeast/southwest trend of the major geologic terrains of the Korean Peninsula, it coincides to a certain degree with the surface topography. The central depression of the Moho interface is co-located with the Yeongnam Massif, which may indicate isostatic compensation for this mountain range (Kwon and Yang, 1985; Choi and Shin, 1996). In contrast, the Gyeonggi Massif in the northeast is located over a shallow section of the crust, requiring a different mechanism to compensate for the uplift. The observed thinning of the crust could result in stronger influences of mantle dynamics on crustal structures in this region. However, to determine the mechanism most plausible for the uplift of the Gyeonggi Massif requires a detailed tomographic study, which will be performed in the second phase of this project.

CONCLUSIONS AND RECOMMENDATIONS

The presented results are corroborated by the studies of Chang and Baag (2006), Herrmann et al. (2006) and Yoo et al. (2007), who mapped the Moho interface using surface-wave dispersion and receiver-function analysis. In both studies, a pattern of the Moho interface, similar to the one displayed in Figures 2 and 4, was found. The present study is complementary to the earlier works, in that a different method and a different dataset generated comparable results.

ACKNOWLEDGEMENTS

The figures and maps throughout this document were created using the Generic Mapping Tools by Wessel and Smith (1995).

REFERENCES

- Chang, S. J. and C. E. Baag (2006). Crustal Structure in South Korea from Joint Analysis of Broadband Waveforms and Travel Times, *Bull. Seis. Soc. Am.* 96: 856–870, doi:10.1785/0120040165.
- Choi, K. S. and Y. H. Shin (1996). Isostasy in and around the Korean Peninsula by analyzing gravity and topography data, *J. Geol. Soc. Korea* 32: 407–420.
- Herrmann R. B., Y. S. Jeon, H. J. Yoo, K. H. Cho, W. R. Walter, and M. Pasyanos (2006). Seismic source and path calibration in the Korean Peninsula, Yellow Sea, and Northeast China, in *Proceedings of the 28th Seismic Research Review on Ground Based Nuclear Explosion Monitoring Technologies*, LA-UR-06-5471, Vol. 1, pp. 60–70.

Kwon, B. D. and S. Y. Yang (1985). A study on the crustal structure of the southern Korean Peninsula through gravity analysis, *J. Korean Inst. Mining Geol.* 18: 309–320.

Wessel, P. and Smith, W. (1995). New version of the generic mapping tools released. *EOS Trans. AGU* 76: 329.

Yoo, H. J., R. B. Herrmann, K. H. Cho, and K. Lee (2006). Imaging the three-dimensional crust of the Korean Peninsula by joint inversion of surface-wave dispersion and teleseismic receiver functions, *Bull. Seism. Soc. Am.* 97: 1001–1011.

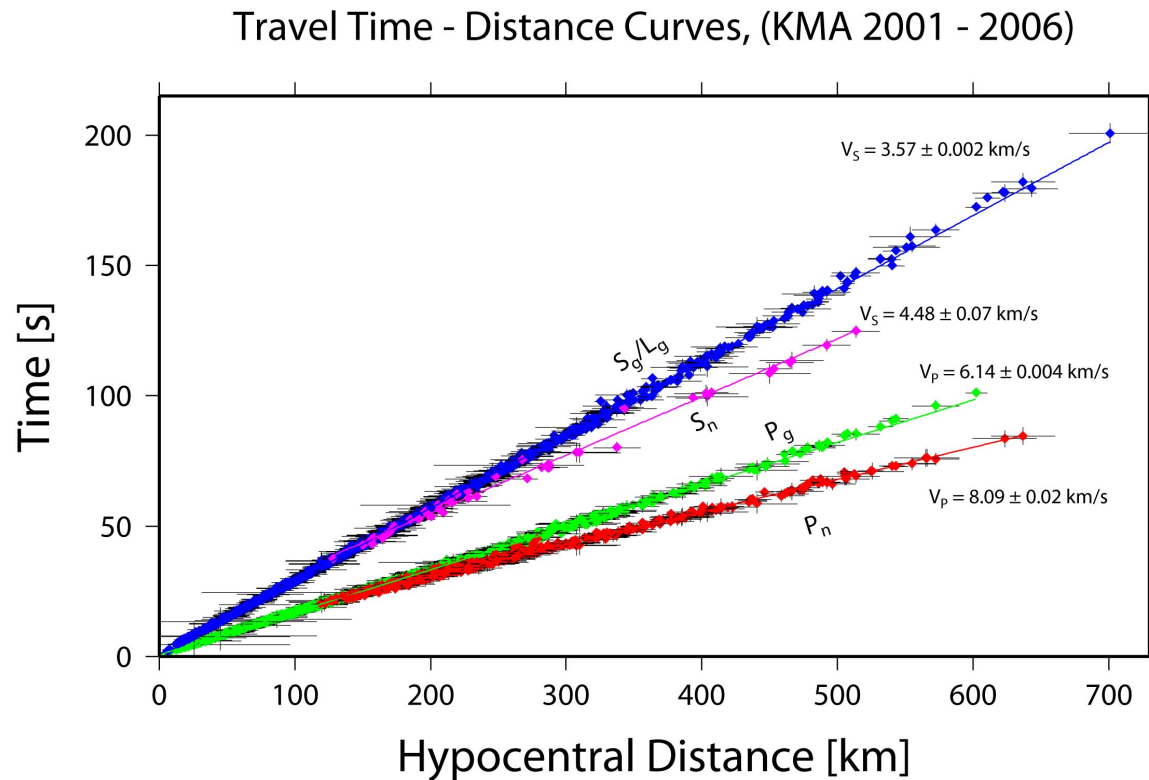


Figure 1. Travel-time as a function of hypocentral distance for the P- and S-wave phase picks as determined from KMA waveform data for the period 2001-2006. The phase picks are indicated by colored diamonds, while the solid colored lines represent their best least-squares fit resulting in the velocity values as noted. The short black horizontal lines at each data point represent the relative location error for each hypocenter estimate associated with that phase pick. The short black vertical lines at each data point represent the relative timing error for event time associated with that phase pick.

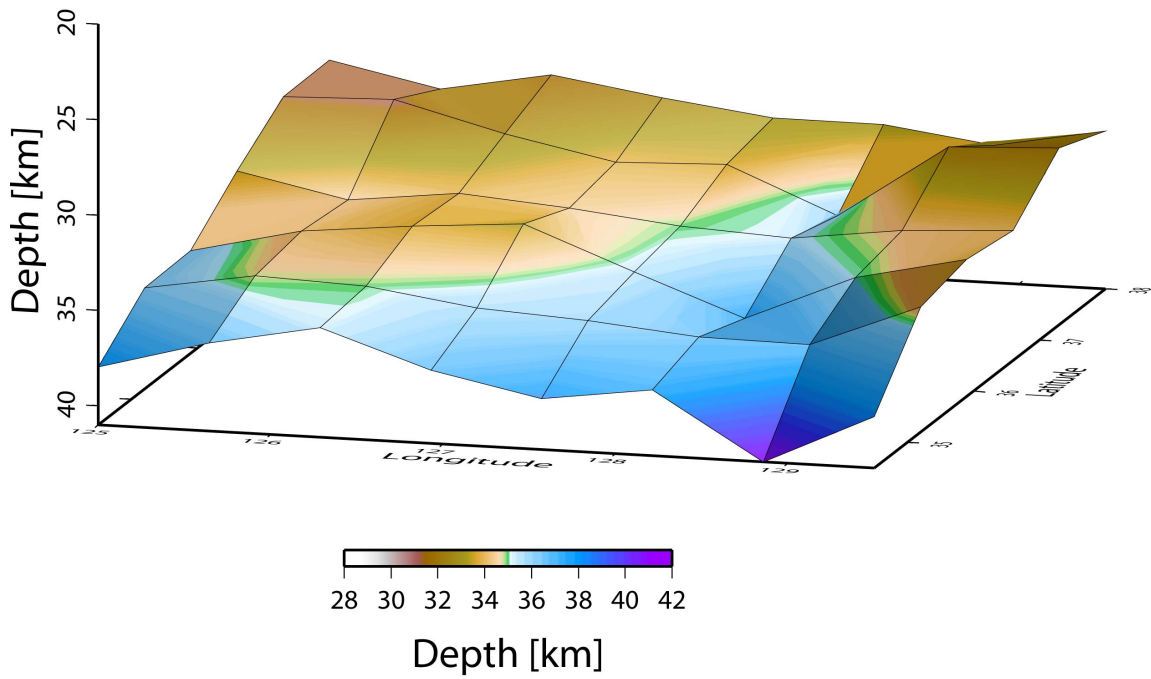


Figure 2. Three-dimensional surface plot of the Moho discontinuity below South Korea. The mapped surface is based on P-wave refraction data recorded by the KMA from 2001 to 2006.

P-Wave Ray Coverage, KMA 2001-2006

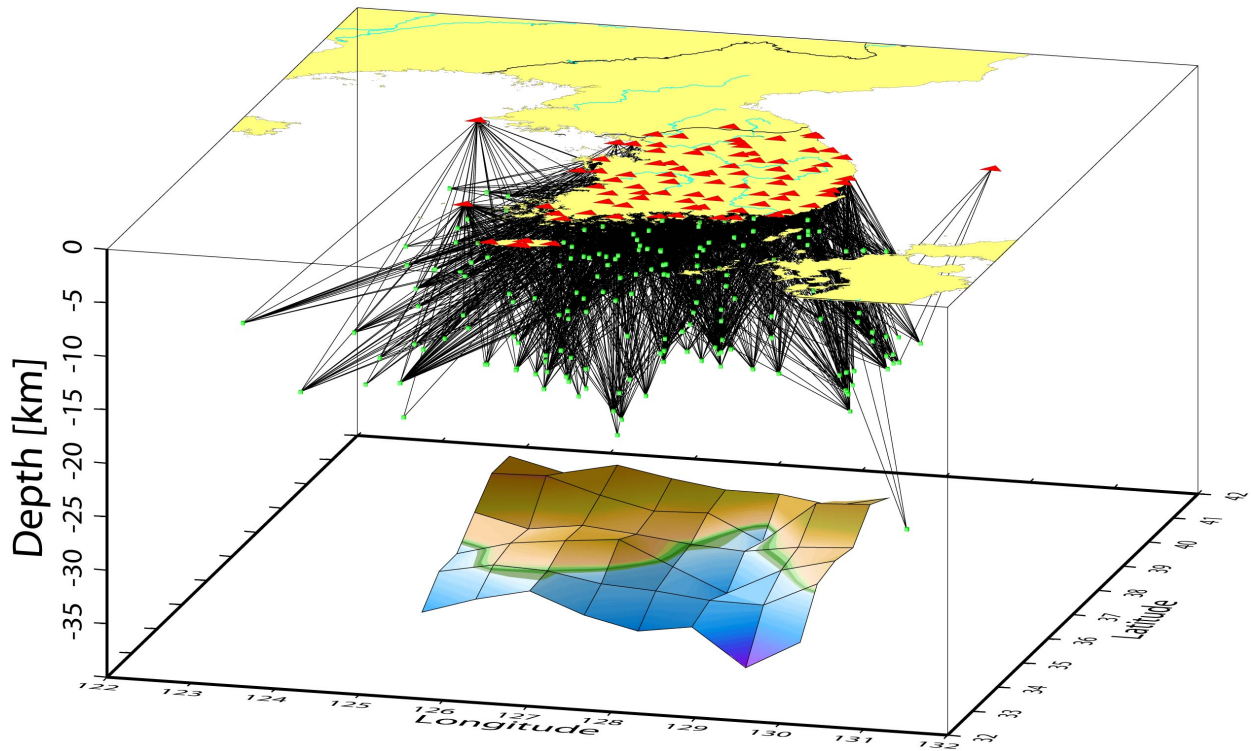


Figure 3. Three-dimensional image of the Moho topography and seismicity below South Korea from the analysis of KMA data for the period 2001-2006. Epicenters are indicated by green circles, seismic stations by red triangles along the surface, and the 3-d P-wave ray coverage by black lines. Vertical exaggeration is greater than 23:1.

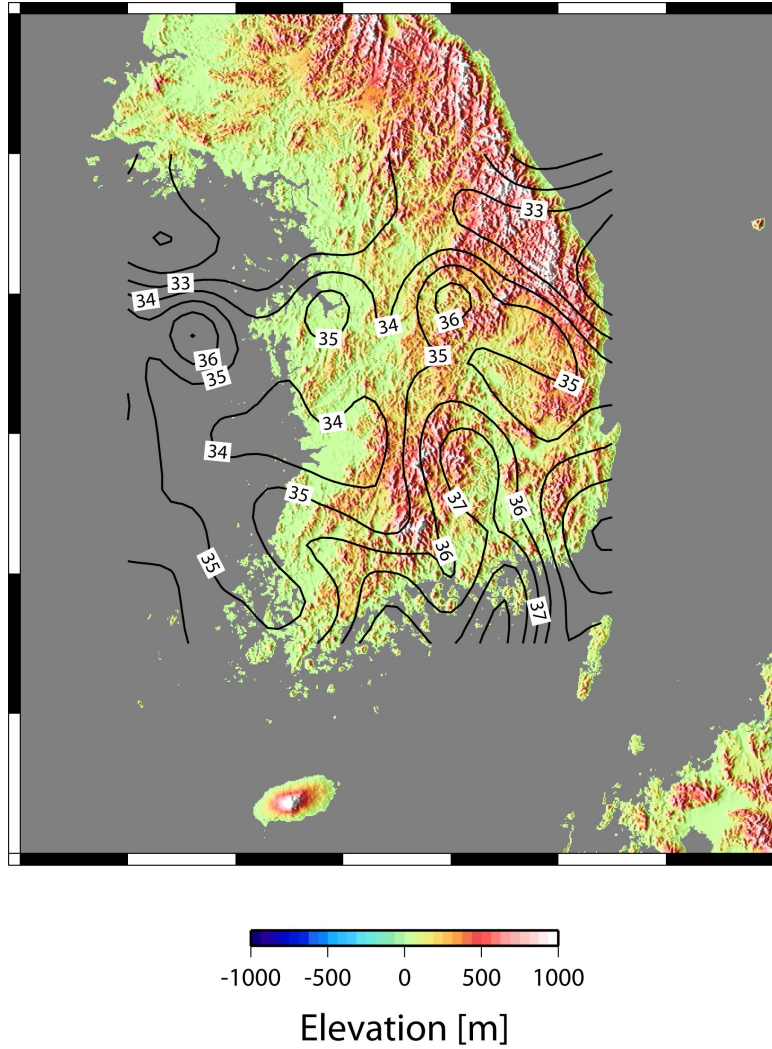


Figure 4. Contour map of the Moho interface below South Korea superimposed on a topography map of the Korean Peninsula. Contour intervals are in kilometers. The contoured surface is based on P-wave refraction data recorded by the KMA from 2001 to 2006.